JBC Papers in Press. Published on December 8, 2016 as Manuscript M116.764712
The latest version is at http://www.jbc.org/cgi/doi/10.1074/jbc.M116.764712

Protein O-linked Mannose β-1,4-N-acetylglucosaminyltransferase 2 (POMGNT2) is a Gatekeeper Enzyme for Functional Glycosylation of α-Dystroglycan

Stephanie M. Halmo[1,2], Danish Singh[1,2], Sneha Patel[1], Shuo Wang[1], Melanie Edlin[1,3], Geert-Jan Boons[1,3], Kelley W. Moremen[1,2], David Live[1], and Lance Wells[1,2,*]

[1]Complex Carbohydrate Research Center, [2]Department of Biochemistry and Molecular Biology, and [3]Department of Chemistry, University of Georgia, Athens, Georgia, 30602, USA

Running title: *POMGNT2, a gatekeeper enzyme*

[*]To whom correspondence should be addressed: Lance Wells, Department of Biochemistry, University of Georgia, Complex Carbohydrate Research Center, 315 Riverbend Road, Athens, Georgia, 30602; Telephone: (706)542-9741; E-mail: lwells@ccrc.uga.edu

Keywords: glycobiology, glycoprotein, dystroglycan, glycosyltransferase, enzyme kinetics, congenital muscular dystrophy, O-mannosylation

ABSTRACT

Disruption of the O-mannosylation pathway involved in functional glycosylation of α-dystroglycan gives rise to congenital muscular dystrophies. Protein O-linked mannose β-1,4-N-acetylglucosaminyltransferase 2 (POMGNT2) catalyzes the first step towards the functional matriglycan structure on α-dystroglycan that is responsible for binding extracellular matrix proteins and certain arenaviruses. Alternatively, protein O-linked mannose β-1,2-N-acetylglucosaminyltransferase 1 (POMGNT1) catalyzes the first step towards other various glycan structures present on α-dystroglycan of unknown function. Here, we demonstrate that POMGNT1 is promiscuous for O-mannosylated peptides while POMGNT2 displays significant primary amino acid selectivity near the site of O-mannosylation. We define a POMGNT2 acceptor motif, conserved among fifty-nine vertebrate species, in α-dystroglycan that when engineered into a POMGNT1-only site is sufficient to convert the O-mannosylated peptide to a substrate for POMGNT2. Additionally, an acceptor glycopeptide is a less efficient substrate for POMGNT2 when two of the conserved amino acids are replaced. These findings begin to define the selectivity of POMGNT2 and suggest this enzyme functions as a gatekeeper enzyme to prevent the vast majority of O-mannosylated sites on proteins from becoming modified with glycan structures functional for binding LG-domain containing proteins.

INTRODUCTION

Congenital muscular dystrophy (CMD) describes a family of genetic, degenerative diseases characterized by contractures, myopathy, and in some cases, central nervous system abnormalities. Many CMDs are caused by defects in the formation of a functional dystrophin glycoprotein complex (DGC) that links the actin cytoskeleton to the extracellular matrix (ECM). α-Dystroglycan (α-DG), encoded by the *DAG1* gene, provides the physical link to LG-domain containing proteins in the ECM (1), however, there are only a few known mutations in the DAG1 coding sequence that lead to CMD (2). A subset of CMDs, termed secondary dystroglycanopathies, is caused by mutations in genes encoding enzymes responsible for glycosylating α-DG in its mucin-like domain (residues 313-489). These secondary dystroglycanopathies range in severity from mild Limb-Girdle muscular dystrophy to the more severe Walker-Warburg syndrome (3-5). The causal genes for secondary dystroglycanopathies have been identified as encoding enzymes in the pathway associated with the biosynthesis of the O-mannosyl (O-Man) glycans (6,7).

The O-mannosylation pathway begins in the endoplasmic reticulum (ER) where a complex of POMT1 and POMT2 catalyze the transfer of mannose from dolicholphosphomannose to serine and threonine residues in an α-linkage to α-DG (8), and presumably a handful of other proteins (9). Bifurcation of the pathway then occurs by the

addition of an N-acetylglucosamine in either a β2 or a β4 linkage (Figure 1). Two enzymes, POMGNT1 and POMGNT2, mediate these additions, respectively. In most cases on α-DG, a β-1,2 linked GlcNAc residue can be added to the initial mannose residue by POMGNT1 in the *cis*-Golgi (10). This core M1 structure can be branched by another GlcNAc addition to give rise to the core M2 glycan structure (11). Much more rarely on α-DG, POMGNT2 will add a β-1,4 linked GlcNAc to the initial mannose residue in the ER, leading to the formation of the core M3 glycan structure (Figure 1).

After POMGNT2 mediated β-1,4 GlcNAc addition, the glycan is subject to further extension with a β-1,3 linked N-acetyl galactosamine (GalNAc) by B3GALNT2 and phosphorylation of the reducing-end mannose at the 6-position by POMK to give rise to the phosphotrisaccharide core M3 glycan structure while still in the ER (12-14). From here, it has been recently demonstrated that Fukutin (FKTN) and Fukutin-related protein (FKRP) appear to be responsible for extending the core M3 phosphotrisaccharide in the Golgi by addition of two ribitol-phosphate units in phosphodiester linkages (15). TMEM5 then apparently adds a xylose (Xyl) to the distal ribitol that is followed by B4GAT1-catalyzed addition of glucuronic acid (GlcA) in a β-1,4 linkage to the xylose (16,17). This primer permits LARGE1 to catalyze the addition of a repeating disaccharide (α-1,3 linked Xyl – β-1,3 linked GlcA) that is the functional component, termed matriglycan, responsible for binding to laminin globular (LG) domains of ECM proteins (2,18,19).

Human α-DG has at least 25 O-mannosylation sites (20-22). The majority of the O-mannosylation sites on α-DG are populated by core M1 and M2 glycan structures via the action of POMGNT1 (M1) followed by MGAT5B (M2) (20-23). Site-mapping studies have identified only two positions, Thr317 and Thr379, on α-DG with M3 core structures, though some evidence suggests 319 and 381 may also be sites of M3 modification (Figure 1) (12,18,20,21). Paradoxically from a spatial-temporal perspective, O-Man modified α-DG encounters POMGNT2 in the ER before POMGNT1 in the *cis*-Golgi yet is preferentially modified by POMGNT1. This led us to hypothesize that POMGNT2 must demonstrate substrate selectivity beyond simply an O-Man modified amino acid.

Here, we explore the specificity of POMGNT2, and compare it with POMGNT1. We synthesized multiple O-mannosylated peptides derived from known M1 and M3 modified sites of α-DG and tested their ability to be acceptor substrates for the two enzymes. POMGNT2 displays selectivity based on the primary amino acid sequence in proximity to the site of O-mannosylation while POMGNT1 is promiscuous. We identified a sequence motif, highly conserved in vertebrates, in α-DG that appears to modulate POMGNT2 substrate specificity *in vitro*. We demonstrated sufficiency of the extended motif by engineering the sequence into a typical M1 O-mannosylated peptide that resulted in it being a POMGNT2 acceptor. We also demonstrate that replacement of conserved amino acids compromises an M3 peptide for extension by POMGNT2. Intriguingly, a conservative degenerate sequence based on our identified motif is present in several human membrane/secreted proteins.

RESULTS

Acceptor Selectivity of POMGNT1 and POMGNT2 using Synthetic α-DG Glycopeptides

In order to identify primary amino acid determinants of POMGNT2 selectivity, we used solid-phase peptide synthesis to generate synthetic glycopeptides whose sequences are those from known O-mannosylated regions of human α-DG (Table 1). Direct physical evidence for core M3 extension at position 379 in α-DG has previously been shown (24), while the threonine at position 341 in α-DG has been demonstrated as a POMT1/POMT2 acceptor that does not carry an M3 core (25). We selected these two sites (379 and 341) because we predicted their extensions differ in core glycan structure while their immediate primary amino acid sequences share a similar Thr(-O-Man)-Pro-Thr (TPT) motif. The synthetic glycopeptides were designed to be 21 amino acids in length with the mannosylated threonine as the central residue (residue 11) to evaluate nearby C-terminal and N-terminal amino acid determinants (Table 1).

To establish if the synthetic glycopeptides were substrates for POMGNT1 and POMGNT2,

we performed overnight radioactive transfer assays. Recombinant human POMGNT1 catalyzed GlcNAc transfer to both the Man341 and Man379 synthetic glycopeptides (Figure 2A, B). To confirm the composition of POMGNT1 reaction products, parallel transfer assays using non-radiolabeled UDP-GlcNAc were performed using the Man341 and Man379 glycopeptides as acceptor substrates, and the reaction products were analyzed by mass spectrometry (MS) (Figure 2C, D). The observed peaks at 859.121 and 899.504 *m/z* in the full FTMS correspond to the addition of a HexNAc residue [+203] to the Man341 and Man379 glycopeptides, respectively. Thus, POMGNT1 will extend the mannose in synthetic glycopeptides at positions 341 and 379 of the α-DG sequence, *in vitro*. These results clearly demonstrate that POMGNT1 exhibits minimal acceptor selectivity between core M1 and M3 sites on these two α-DG-derived glycopeptides.

In comparison, POMGNT2 showed preferential acceptor selectivity for the known M3 site in the α-DG sequence. Radiolabel transfer assays showed no detectable transfer of the sugar to the acceptor Man341 glycopeptide by POMGNT2 (Figure 2A) but transfer of GlcNAc to the Man379 synthetic glycopeptide (Figure 2B). Parallel non-radioactive transfer assays followed by MS analysis identified the composition of the POMGNT2 reaction products and verified the transfer results observed in the radioactive assays (Figure 2E, F). The predominant peak at 791.427 *m/z* in the full FTMS corresponds to the unmodified Man341 glycopeptide with a single mannose (Figure 2E). In contrast to the results seen in Figure 2E, the observed peak at 899.504 *m/z* in the full FTMS in Figure 2F corresponds to the addition of a HexNAc residue [+203] to the Man379 glycopeptide. These results suggest that POMGNT2 preferentially modifies specific sites on α-DG intended for core M3 glycan elaboration.

Kinetic Parameters of POMGNT1 and POMGNT2 with Synthetic α-DG Glycopeptides

To further characterize the substrate specificities of POMGNT1 and POMGNT2, additional core M1 and core M3 synthetic glycopeptides were generated. Man414 and Man317 are known O-mannosylated regions of α-DG (18,21). Evidence for core M3 extension at position 317 in α-DG has been shown previously (12,18). Man317 is 21 amino acids in length, contains the TPT motif, and has the mannosylated threonine as the central residue (residue 11), similar to Man379 and Man341 (Table 1). Man414 is only 7 amino acids in length, and lacks the TPT motif (Table 1). However, the kinetics of Man414 with POMGNT1 has previously been studied (26) and the homologous residue in rabbit (*Oryctolagus cuniculus)* has been site-mapped with mannose (21) making it a useful predicted core M1 glycopeptide for this study.

Glycosyltransferase reaction kinetics for POMGNT1 with the four synthesized glycopeptides were investigated by UDP-Glo™ assays. The α-DG sequences in the four synthetic glycopeptides were all utilized by POMGNT1 as acceptors (Figure 3A-D). Inspection of the K_m values derived from nonlinear regression analyses of the experimentally obtained values reveals that the affinity of POMGNT1 for synthetic acceptor glycopeptides containing a TPT motif (Man317, Man379, Man341) is greater than the affinity for the Short Man414 synthetic glycopeptide lacking a TPT motif (Table 1). POMGNT1 has the fastest turnover (k_{cat}) with the Man341 synthetic glycopeptide, but catalytic efficiency (k_{cat}/K_m) is an order of magnitude greater for the core M3 synthetic glycopeptides, Man317 and Man379 (Table 1).

To validate the acceptor selectivity of POMGNT2, we also performed UDP-Glo™ assays with the four synthesized glycopeptides to investigate glycosyltransferase reaction kinetics. Transfer of GlcNAc to Man341 and Man414 by POMGNT2 (Figure 4A,C) was below the level of detection, while Man379 and Man317 (Figure 4B, D) are clearly acceptor substrates for POMGNT2 activity. The measured K_m, k_{cat}, and k_{cat}/K_m for Man317 and Man379 synthetic glycopeptides with POMGNT2 are similar (Table 1). These data are consistent with the results obtained in our initial transfer assays and support the proposal that the features of the primary amino acid sequence in the region of the TPT sequence are determinants of POMGNT2 selectivity.

A Primary Amino Acid Motif in α-DG is Favorable for POMGNT2 Activity

It was previously suggested that all O-mannosylated sites on α-DG have a conserved Thr-Pro-Thr (TPT) motif at the mannosylated

threonine (18,25) though site mapping studies have demonstrated that only a subset of mapped sites follow this pattern (20-22). Indeed, the primary amino acid sequences around mapped O-mannose sites on α-DG (excluding sites Thr317 and Thr379) are heterogeneous (Figure 5A). To identify primary sequence elements that govern the observed preferences on POMGNT2 acceptor substrate selectivity, α-DG amino acid sequences surrounding sites Thr317 and Thr379 from fifty-nine vertebrate species with orthologues of human DAG1, POMGNT1 or POMGNT2, and FKTN or B4GAT1 were aligned using WebLogo (27) (Figure 5B). The previously identified TPT motif was evident in our alignment, but other conserved amino acids were observed that are not present around Thr341. Interestingly, our alignment of 317/379 M3 sites across species demonstrated that arginines at -6 and -8 and an Ile at -3 were conserved in addition to the P at +1 and the T at +2. Thus, the R-X-R-X-X-I-X-X-T-P-T motif is a proposed conserved sequence for M3 extension (Figure 5B).

Since this motif is only present at known core M3 sites and not at core M1 sites, we hypothesized that the R-X-R portion of the primary amino acid sequence motif of α-DG might confer extension by POMGNT2. To test this, we synthesized a modified version of the Man341 peptide that already contains the TPT sequence and an Ile at -3, that we refer to as Man341-RPR. In this glycopeptide, we replaced the two divergent amino acids at -6 and -8 with arginines to introduce the conserved R-X-R motif. Glycosyltransferase reaction kinetics of POMGNT2 with this modified glycopeptide was investigated by UDP-Glo™ assay. In contrast to the undetectable reaction with Man341, POMGNT2 transferred GlcNAc to Man341-RPR (Figure 6A, Table 1). Thus, we successfully converted a core M1 non-acceptor peptide into a core M3 acceptor for POMGNT2 *in vitro* by the addition of our identified motif.

To further test that the R-X-R portion of the primary amino acid sequence motif of α-DG is important for glycan extension by POMGNT2, we synthesized a new glycopeptide based on the sequence at a known core M3 site (379) but with the two N-terminal arginine residues altered to the divergent residues of a core M1 acceptor (Man341). We have designated this modified core M3 glycopeptide as Man379-ETP. Glycosyltransferase reaction kinetics of POMGNT2 with this modified glycopeptide were investigated by UDP-Glo™ assays. In comparison to the kinetics of POMGNT2 with Man379, POMGNT2 has a lower affinity and a greater than five-fold reduction in catalytic efficiency for Man379-ETP (Figure 6B, Table 1). The replacement of our identified R-X-R motif in a core M3 acceptor with divergent residues reduced but did not eliminate POMGNT2 activity.

Lastly, to test the necessity of the R-X-R portion of the primary amino acid sequence motif of α-DG for POMGNT2 activity, we synthesized a truncated version of the Man379 M3 glycopeptide we refer to as ShortMan379. The N-terminus of this glycopeptide begins immediately following the R-X-R motif. Glycosyltransferase reaction kinetics of POMGNT2 with this truncated glycopeptide were investigated by the UDP-Glo™ assay. POMGNT2 utilized ShortMan379 as an acceptor substrate with a similar affinity to Man379 but with a less than one-fold reduction in catalytic efficiency (Figure 6C, Table 1). Thus, the R-X-R portion of the motif appears to not be essential in the context of a synthetic peptide for POMGNT2 activity.

DISCUSSION

While POMGNT2 is poised to modify α-DG in the ER before it encounters POMGNT1 in the *cis*-Golgi, only two M3 sites have been identified on α-DG. Thus, it seems likely that POMGNT2 demonstrates acceptor substrate preferences beyond simply an O-Man modified residue. We tested this hypothesis regarding specificity by examining the impact of local primary amino acid sequence around O-Man sites on synthetic peptides as acceptor substrates for POMGNT1 and POMGNT2.

Employing a set of O-Man glycopeptide substrates, we have shown that POMGNT2 has a preference for acceptors with mannosylated residues at positions Thr317 and Thr379 while POMGNT1 has no significant acceptor substrate preferences among the various synthetic glycopeptides tested (Figure 2-4 and Table 1). Analysis of the sites that are POMGNT2-dependent demonstrate a R-X-R-X-X-I-X-X-T-P-T motif that is conserved among vertebrata α-DG (Figure 5B). We also observed that this sequence

is not found in any of the mapped sites from other O-mannosylated proteins (9) consistent with α-DG being the only demonstrated protein to contain M3 glycans (Figure 5A). We found that replacement of a divergent sequence on a POMGNT1 acceptor that was only missing the conserved R-X-R motif converted it to a POMGNT2 acceptor, demonstrating that replacing the two amino acids was sufficient to confer activity (Figure 6A). Likewise, replacement of the arginines in the Man379 peptide with amino acids found in the M1 peptide of Man341 reduced the efficiency of POMGNT2 to catalyze the addition of GlcNAc to the O-Man peptide more than five-fold (Figure 6B). However, while the addition of the R-X-R motif to a core M1 acceptor is sufficient to make it a substrate for POMGNT2, the complete removal of the R-X-R motif on a core M3 acceptor does not abolish POMGNT2 activity (Figure 6C). Taken together, this suggests that the R-X-R motif allows for extension by POMGNT2 at core M3 sites, but is not essential for a short synthetic O-Man peptide. These results support a case of sufficiency in the absence of necessity which deviates from the normal necessary and sufficient or necessary but not sufficient arguments. We would rationalize that when there is sequence upstream of the site of action, as that actually found in the full-length alpha-dystroglycan protein, that non-basic amino acids replacing the R-X-R portion of the motif generate steric or electrostatic clashes that prevent proper binding of the substrate protein.

Interestingly for Man317, the identified R-X-R motif is upstream of the known Furin cleavage site. However, as POMGNT2 is an ER-resident glycosyltransferase and Furin is located in the Golgi, POMGNT2 acts first and thus has the capability to interact with residues upstream of the Furin cleavage site and this may at least partially explain the requirement for the N-terminus for synthesis of functionally glycosylated mature α-DG (19).

Our current model, based on the data presented here, is that POMGNT2 selectivity determines which sites on α-DG become modified with the core M3 glycan structure. In turn, only the core M3 glycan structure can be extended by B3GALNT2, phosphorylated by POMK and further elaborated to become the functional matriglycan for α-DG (2,13). Functional glycosylation of α-DG, and, in particular, matriglycan synthesis stemming from the POMGNT2-dependent core M3 glycan structure is required for binding to extracellular matrix (ECM) proteins with laminin globular domains and maintaining overall ECM integrity (11). Thus, POMGNT2 acts a *gatekeeper enzyme* for functional glycosylation of α-DG.

The strict R-X-R-X-X-I-X-X-T-P-T motif that we have presented here is not present on any other secreted or membrane associated protein in humans except for α-DG at T317/319 and T379/381 (2,13). Relaxing the sequence constraints to allow for conservative replacements generates a motif of R/K-X-R/K-X-X-I/L/V-X-X-T/S-P-T/S. This motif is found on a handful of membrane/secreted human proteins including SRPX, CLEC18C, FREM2, MANBA, SEMA3E, SPACA7, and TMEM182. However, if we examine conservation of the motif in these proteins across 59 vertebrate species, as we did for α-DG, we see poor conservation (data not shown). This lends further support to the working model that only α-DG contains sequences that are substrates for POMGNT2 that go on to become functionally glycosylated with matriglycan (2).

We have identified and partially characterized a primary amino acid sequence motif governing acceptor specificity for POMGNT2 towards O-mannosylated substrates. Additional studies are required to fully characterize the functional roles of individual amino acids in this motif. Structural analyses of POMGNT2 in complex with various acceptor substrates would greatly assist in defining the molecular details of the POMGNT2 *gatekeeping* mechanism that we have established here. Furthermore, future *in vivo* studies testing the role of the R-X-R-X-X-I-X-X-T-P-T motif in POMGNT2 acceptor selectivity will be invaluable to complement our *in vitro* findings presented here.

EXPERIMENTAL PROCEDURES

Cell Culture and Protein Purification

The catalytic domains of human POMGNT1 (amino acid residues 60–660, UniProt Q8WZA1) and POMGNT2 (amino acid residues 25–580, UniProt Q8NAT1) were expressed as soluble, secreted fusion proteins by transient transfection of HEK293 suspension cultures (28).

The coding regions were amplified from Mammalian Gene Collection (29) clones using primers that appended a tobacco etch virus (TEV) protease cleavage site (30) to the NH_2-terminal end of the coding region and attL1 and attL2 Gateway adaptor sites to the 5′ and 3′ terminal ends of the amplimer products. The amplimers were recombined via BP clonase reaction into the pDONR221 vector and the DNA sequences were confirmed. The pDONR221 clones were then recombined via LR clonase reaction into a custom Gateway adapted version of the pGEn2 mammalian expression vector (28,31) to assemble a recombinant coding region comprised of a 25 amino acid NH_2-terminal signal sequence from the *T. cruzi* lysosomal α-mannosidase (32) followed by an 8xHis tag, 17 amino acid AviTag (33), 'superfolder' GFP (34), the nine amino acid sequence encoded by attB1 recombination site, followed by the TEV protease cleavage site and the respective glycosyltransferase catalytic domain coding region. Suspension culture HEK293f cells (Life Technologies, Grand Island, NY) were transfected as previously described (28) and the culture supernatant was subjected to Ni-NTA superflow chromatography (Qiagen, Valencia, CA). Enzyme preparations eluted with 300 mM imidazole were concentrated to ~1 mg/ml using an ultrafiltration pressure cell membrane (Millipore, Billerica, MA) with a 10 kDa molecular weight cutoff.

Glycopeptide Synthesis

The glycopeptide synthesis here extends earlier work describing synthesis of O-Man-Ser and -Thr peptide synthesis building blocks, as well as O-Man glycopeptides (35). The glycopeptides were prepared as C-terminal carboxamides and acetylated at the N-terminus to emulate the situation in the native protein. For this work all couplings except those for glycosylated residues were carried out on an automated microwave-assisted solid-phase peptide synthesizer (Liberty CEM Microwave Synthesizer) using standard protocols in the instrument software, on Rink amide resin (~0.5 meq/gm, Novabiochem) via an N^R-Fmoc-based approach with DMF as the primary solvent. 20% 4-methyl piperidine in DMF was used for Fmoc removal. 2-(1H-benzotriazole-1-yl)-oxy-1,1,3,3-tetramethyluronium hexafluorophosphate (HBTU)/1-hydroxybenzotriazole (HOBt) in the presence of N,N-diisopropylethylamine (DIPEA) were employed as the coupling reagents for standard amino acids. For the coupling of the glycosylated amino acid, Fmoc-Thr(α-D-Man(Ac)$_4$)-OH (Sussex Research), the peptide resin was removed from the synthesizer and coupling performed manually using a CEM Discover microwave apparatus. 2-(7-aza-1H-benzotriazole-1-yl)-1,1,3,3-tetramethyluronium hexafluorophosphate (HATU)/ 1-hydroxy-7-azabenzotriazole (HOAt) in the presence of DIPEA were the activating reagents. Typically two couplings at ~1.5 fold excess of glycosylated amino acid to the resin loading were done for this amino acid to conserve reagent. Upon completion of the manual coupling reaction, as determined by Matrix-assisted laser desorption/ionization-time of flight mass spectrometry (MALDI-TOF MS), glycopeptide resins were returned to the automatic synthesizer to complete assembly. After final N-deprotection, the glycopeptides were manually N-acetylated by treatment with DMF/Acetic Anhydride/DIPEA 85/10/5 v/v for ~30 min, and the O-acetyl protection on the mannosyl residues were subsequently removed by two successive treatments with Hydrazine/MeOH 70/20 v/v for an hour each. Glycopeptides were then cleaved from the resin as C-terminal carboxamides, with simultaneous removal of remaining amino acid side chain protection through treatment with TFA/TIPS/H_2O 95/2.5/2.5 for ~4 hrs. The resin was filtered off and the TFA solution concentrated on a rotary evaporator to a few mL. The remaining concentrate was added drop wise to cold ether from which the crude glycopeptides precipitated. After centrifugation and removal of the ether supernatant, the glycopeptides were redissolved and purified via HPLC over an Ultra II 250x10.0mm 5µm C_{18} column (RESTEK) with a 0.1% TFA in water/0.1% TFA in Acetonitrile solvent gradient. Purity was verified by analytical HPLC and MALDI-TOF MS (see Supplementary Figure 1). Yields were in the range of 30 -50%.

Radiolabel Transfer Assays

The radiometric assays were carried out in reactions containing 100 mM MES (pH 6.5), 10 mM $MnCl_2$, 2 mM UDP-GlcNAc mixed with 10nCi ^{3}H-UDP-GlcNAc, and 1mM glycopeptide acceptor. Reactions were incubated for 21 hrs at

37°C, then quenched by addition of 5 µl 1% TFA and boiled at 100°C for 5 min. Reaction products were purified by reverse phase separation using C_{18} SepPak micro spin columns (The Nest Group) by loading and washing with 0.1% formic acid and elution with 80% acetonitrile with 0.1% formic acid. Disintegrations per minute (DPMs) were counted using a liquid scintillation counter (Beckman) to determine the amount of ^{3}H-GlcNAc incorporated into the glycopeptides. The data presented represent the average of at least 3 independent experiments.

Mass Spectrometry

Cold glycosyltransferase reactions used for analysis by mass spectrometry were carried out identical to the radioactive transfer assays but without radioactive UDP-GlcNAc. After reverse phase separation, the product was vacuumed to dryness and resuspended in 100 µl of 0.1% formic acid. Samples were filtered using a 0.2 µm nanosep microcentrifuge filter (Pall Life Sciences) and transferred to an autosampler vial with glass insert (Thermo Scientific). The samples were run on a Thermo Scientific™ Orbitrap Fusion™ Lumos™ mass spectrometer. Full Fourier transform MS Spectra were analyzed using Xcalibur Qual Browser software, and MS/MS scans were analyzed using Byonic™ Version 2.6.46 (Protein Metrics Inc.), using a precursor mass tolerance of 10 ppm and a fragmentation mass tolerance of 0.3 Daltons followed by manual interpretation.

UDP-Glo™ Glycosyltransferase Assays

UDP-Glo™ Glycosyltransferase Assays (Promega) were performed using 50 mM Tris-HCl (pH 7.5), 5 mM $MnCl_2$, 100 µM UDP-GlcNAc, 40 ng of enzyme, and varying amounts of glycopeptide acceptor-substrates at 37°C for 2 hrs in a white, flat bottom, 384-well plate. After the glycosyltransferase reaction, an equal volume of UDP Detection Reagent was added to simultaneously convert the UDP product to ATP and generate light in a luciferase reaction. The light generated was detected using a GloMax-Multi+ luminometer (Promega). Luminescence was correlated to UDP concentration by using a UDP standard curve. Kinetic parameters were extracted from the data after fitting to the Michaelis-Menten equation using the non-linear regression fit in GraphPad Prism Version 7.1. The data presented represent the average of at least 3 independent experiments.

WebLogo Consensus Sequence Alignment

All vertebrate species available on the Ensembl genome browser (release 85) (36) with orthologues of human DAG1, POMGNT1 or POMGNT2, and FKTN or B4GAT1 (*X. tropicalis, L. chalumnae, A. carolinensis, C. hoffmanni, T. truncatus, P. sinensis, M. gallopavo, G. gallus, A. platyrhynchos, T. guttata, F. albicollis, D. ordii, E. telfairi, O. princeps, L. africana, P. capensis, M. lucifugus, C. porcellus, R. norvegicus, M. musculus, E. europaeus, D. novemcinctus, O. garnettii, I. tridecemlineatus, B. taurus, O. aries, O. cuniculus, M. putorius furo, C. lupus familiaris, F. catus, A. melanoleuca, T. syrichta, T. belangeri, P. vampyrus, S. scrofa, E. caballus, C. jacchus, P. anubis, M. mulatta, C. sabaeus, N. leucogenys, G. gorilla gorilla, P. troglodytes, H. sapiens, O. anatinus, M. eugenii, M. domestica, S. harrisii, L. oculatus, D. rerio, A. mexicanus, T. nigroviridis, T. rubripes, O. latipes, X. maculatus, P. formosa, G. morhua, G. aculeatus,* and *O. niloticus*) were aligned to human DAG1 using Clustal Omega (37). The ten amino acids upstream and downstream of the Threonine at position 317 and 379 in human DAG1 for all species were extracted from the alignment and used for analysis in Berkeley's WebLogo program (version 3) (27).

ACKNOWLEDGEMENTS

The authors would like to thank M. Osman Sheikh for assistance in the preparation of this manuscript, and Robert Bridger and Jeremy L. Praissman for technical assistance with mass spectrometry. The authors would like to thank all members of the Wells lab for thoughtful discussions. This work was supported in part by grants from the National Institutes of Health (R01GM111939, DL and LW; P01GM107012, GJB, KM, LW; P41GM103490, KM and LW; P41GM103390, KM and DL; S10RR027155 for purchase of the peptide synthesizer, DL). SH is supported in part by a T32 NIH training grant (T32GM107004). The content is solely the responsibility of the authors and does not necessarily represent the official views of the National Institutes of Health.

CONFLICT OF INTEREST

The authors declare that they have no conflicts of interest with the contents of this article.

AUTHOR CONTRIBUTIONS

LW, DL, and KM conceived and coordinated the study. SH and LW wrote the paper. SH, SP,DS, and LW designed, performed and analyzed all experiments shown. SW and KM designed and constructed vectors for expression of proteins. SH, SP and SW expressed and purified protein. ME and SH synthesized the glycopeptides under the direction of DL and GJB. All authors reviewed the results and approved the final version of the manuscript.

REFERENCES

1. Ervasti, J. M., and Campbell, K. P. (1993) A role for the dystrophin-glycoprotein complex as a transmembrane linker between laminin and actin. *The Journal of Cell Biology* **122**, 809-823
2. Yoshida-Moriguchi, T., and Campbell, K. P. (2015) Matriglycan: a novel polysaccharide that links dystroglycan to the basement membrane. *Glycobiology* **25**, 702-713
3. Live, D., Wells, L., and Boons, G.-J. (2013) Dissecting the Molecular Basis of the Role of the O-Mannosylation Pathway in Disease: α-Dystroglycan and Forms of Muscular Dystrophy. *ChemBioChem* **14**, 2392-2402
4. Godfrey, C., Foley, A. R., Clement, E., and Muntoni, F. (2011) Dystroglycanopathies: coming into focus. *Current Opinion in Genetics & Development* **21**, 278-285
5. Voglmeir, J., Kaloo, S., Laurent, N., Meloni, Marco M., Bohlmann, L., Wilson, Iain B. H., and Flitsch, Sabine L. (2011) Biochemical correlation of activity of the α-dystroglycan-modifying glycosyltransferase POMGnT1 with mutations in muscle-eye-brain disease. *Biochemical Journal* **436**, 447-455
6. Jae, L. T., Raaben, M., Riemersma, M., van Beusekom, E., Blomen, V. A., Velds, A., Kerkhoven, R. M., Carette, J. E., Topaloglu, H., Meinecke, P., Wessels, M. W., Lefeber, D. J., Whelan, S. P., van Bokhoven, H., and Brummelkamp, T. R. (2013) Deciphering the Glycosylome of Dystroglycanopathies Using Haploid Screens for Lassa Virus Entry. *Science* **340**, 479-483
7. Wells, L. (2013) The O-Mannosylation Pathway: Glycosyltransferases and Proteins Implicated in Congenital Muscular Dystrophy. *The Journal of Biological Chemistry* **288**, 6930-6935
8. Manya, H., Chiba, A., Yoshida, A., Wang, X., Chiba, Y., Jigami, Y., Margolis, R. U., and Endo, T. (2004) Demonstration of mammalian protein O-mannosyltransferase activity: Coexpression of POMT1 and POMT2 required for enzymatic activity. *Proceedings of the National Academy of Sciences of the United States of America* **101**, 500-505
9. Vester-Christensen, M. B., Halim, A., Joshi, H. J., Steentoft, C., Bennett, E. P., Levery, S. B., Vakhrushev, S. Y., and Clausen, H. (2013) Mining the O-mannose glycoproteome reveals cadherins as major O-mannosylated glycoproteins. *Proceedings of the National Academy of Sciences* **110**, 21018-21023
10. Takahashi, S., Sasaki, T., Manya, H., Chiba, Y., Yoshida, A., Mizuno, M., Ishida, H.-K., Ito, F., Inazu, T., Kotani, N., Takasaki, S., Takeuchi, M., and Endo, T. (2001) A new β-1,2-N-acetylglucosaminyltransferase that may play a role in the biosynthesis of mammalian O-mannosyl glycans. *Glycobiology* **11**, 37-45
11. Praissman, J. L., and Wells, L. (2014) Mammalian O-Mannosylation Pathway: Glycan Structures, Enzymes, and Protein Substrates. *Biochemistry* **53**, 3066-3078
12. Yagi, H., Nakagawa, N., Saito, T., Kiyonari, H., Abe, T., Toda, T., Wu, S.-W., Khoo, K.-H., Oka, S., and Kato, K. (2013) AGO61-dependent GlcNAc modification primes the formation of functional glycans on α-dystroglycan. *Scientific Reports* **3**, 3288
13. Yoshida-Moriguchi, T., Willer, T., Anderson, M. E., Venzke, D., Whyte, T., Muntoni, F., Lee, H., Nelson, S. F., Yu, L., and Campbell, K. P. (2013) SGK196 Is a Glycosylation-Specific O-Mannose Kinase Required for Dystroglycan Function. *Science* **341**, 896-899
14. Ogawa, M., Nakamura, N., Nakayama, Y., Kurosaka, A., Manya, H., Kanagawa, M., Endo, T., Furukawa, K., and Okajima, T. (2013) GTDC2 modifies O-mannosylated α-dystroglycan in the endoplasmic reticulum to generate N-acetyl glucosamine epitopes reactive with CTD110.6 antibody. *Biochemical and Biophysical Research Communications* **440**, 88-93
15. Kanagawa, M., Kobayashi, K., Tajiri, M., Manya, H., Kuga, A., Yamaguchi, Y., Akasaka-Manya, K., Furukawa, J.-i., Mizuno, M., Kawakami, H., Shinohara, Y., Wada, Y., Endo, T., and Toda, T. (2016) Identification of a Post-translational Modification with Ribitol-Phosphate and Its Defect in Muscular Dystrophy. *Cell Reports*

16. Praissman, J. L., Willer, T., Sheikh, M. O., Toi, A., Chitayat, D., Lin, Y. Y., Lee, H., Stalnaker, S. H., Wang, S., Prabhakar, P. K., Nelson, S. F., Stemple, D. L., Moore, S. A., Moremen, K. W., Campbell, K. P., and Wells, L. (2016) The functional O-mannose glycan on alpha-dystroglycan contains a phospho-ribitol primed for matriglycan addition. *Elife* **5**
17. Praissman, J. L., Live, D. H., Wang, S., Ramiah, A., Chinoy, Z. S., Boons, G.-J., Moremen, K. W., and Wells, L. (2014) B4GAT1 is the priming enzyme for the LARGE-dependent functional glycosylation of α-dystroglycan. *eLife* **3**
18. Hara, Y., Kanagawa, M., Kunz, S., Yoshida-Moriguchi, T., Satz, J. S., Kobayashi, Y. M., Zhu, Z., Burden, S. J., Oldstone, M. B. A., and Campbell, K. P. (2011) Like-acetylglucosaminyltransferase (LARGE)-dependent modification of dystroglycan at Thr-317/319 is required for laminin binding and arenavirus infection. *Proceedings of the National Academy of Sciences* **108**, 17426-17431
19. Kanagawa, M., Saito, F., Kunz, S., Yoshida-Moriguchi, T., Barresi, R., Kobayashi, Y. M., Muschler, J., Dumanski, J. P., Michele, D. E., Oldstone, M. B. A., and Campbell, K. P. (2004) Molecular Recognition by LARGE Is Essential for Expression of Functional Dystroglycan. *Cell* **117**, 953-964
20. Nilsson, J., Nilsson, J., Larson, G., and Grahn, A. (2010) Characterization of site-specific O-glycan structures within the mucin-like domain of α-dystroglycan from human skeletal muscle. *Glycobiology* **20**, 1160-1169
21. Stalnaker, S. H., Hashmi, S., Lim, J.-M., Aoki, K., Porterfield, M., Gutierrez-Sanchez, G., Wheeler, J., Ervasti, J. M., Bergmann, C., Tiemeyer, M., and Wells, L. (2010) Site Mapping and Characterization of O-Glycan Structures on α-Dystroglycan Isolated from Rabbit Skeletal Muscle. *The Journal of Biological Chemistry* **285**, 24882-24891
22. Harrison, R., Hitchen, P. G., Panico, M., Morris, H. R., Mekhaiel, D., Pleass, R. J., Dell, A., Hewitt, J. E., and Haslam, S. M. (2012) Glycoproteomic characterization of recombinant mouse alpha-dystroglycan. *Glycobiology* **22**, 662-675
23. Lee, J. K., Matthews, R. T., Lim, J. M., Swanier, K., Wells, L., and Pierce, J. M. (2012) Developmental expression of the neuron-specific N-acetylglucosaminyltransferase Vb (GnT-Vb/IX) and identification of its in vivo glycan products in comparison with those of its paralog, GnT-V. *J Biol Chem* **287**, 28526-28536
24. Yoshida-Moriguchi, T., Yu, L., Stalnaker, S. H., Davis, S., Kunz, S., Madson, M., Oldstone, M. B., Schachter, H., Wells, L., and Campbell, K. P. (2010) O-mannosyl phosphorylation of alpha-dystroglycan is required for laminin binding. *Science* **327**, 88-92
25. Manya, H., Suzuki, T., Akasaka-Manya, K., Ishida, H.-K., Mizuno, M., Suzuki, Y., Inazu, T., Dohmae, N., and Endo, T. (2007) Regulation of Mammalian Protein O-Mannosylation: PREFERENTIAL AMINO ACID SEQUENCE FOR O-MANNOSE MODIFICATION. *Journal of Biological Chemistry* **282**, 20200-20206
26. Mo, K.-F., Fang, T., Stalnaker, S. H., Kirby, P. S., Liu, M., Wells, L., Pierce, M., Live, D. H., and Boons, G.-J. (2011) Synthetic, Structural, and Biosynthetic Studies of an Unusual Phospho-Glycopeptide Derived from α-Dystroglycan. *Journal of the American Chemical Society* **133**, 14418-14430
27. Crooks, G. E., Hon, G., Chandonia, J. M., and Brenner, S. E. (2004) WebLogo: a sequence logo generator. *Genome research* **14**, 1188-1190
28. Meng, L., Forouhar, F., Thieker, D., Gao, Z., Ramiah, A., Moniz, H., Xiang, Y., Seetharaman, J., Milaninia, S., Su, M., Bridger, R., Veillon, L., Azadi, P., Kornhaber, G., Wells, L., Montelione, G. T., Woods, R. J., Tong, L., and Moremen, K. W. (2013) Enzymatic basis for N-glycan sialylation: structure of rat alpha2,6-sialyltransferase (ST6GAL1) reveals conserved and unique features for glycan sialylation. *J Biol Chem* **288**, 34680-34698
29. Gerhard, D. S., Wagner, L., Feingold, E. A., Shenmen, C. M., Grouse, L. H., Schuler, G., Klein, S. L., Old, S., Rasooly, R., Good, P., Guyer, M., Peck, A. M., Derge, J. G., Lipman, D., Collins,

F. S., Jang, W., Sherry, S., Feolo, M., Misquitta, L., Lee, E., Rotmistrovsky, K., Greenhut, S. F., Schaefer, C. F., Buetow, K., Bonner, T. I., Haussler, D., Kent, J., Kiekhaus, M., Furey, T., Brent, M., Prange, C., Schreiber, K., Shapiro, N., Bhat, N. K., Hopkins, R. F., Hsie, F., Driscoll, T., Soares, M. B., Casavant, T. L., Scheetz, T. E., Brown-stein, M. J., Usdin, T. B., Toshiyuki, S., Carninci, P., Piao, Y., Dudekula, D. B., Ko, M. S., Kawakami, K., Suzuki, Y., Sugano, S., Gruber, C. E., Smith, M. R., Simmons, B., Moore, T., Waterman, R., Johnson, S. L., Ruan, Y., Wei, C. L., Mathavan, S., Gunaratne, P. H., Wu, J., Garcia, A. M., Hulyk, S. W., Fuh, E., Yuan, Y., Sneed, A., Kowis, C., Hodgson, A., Muzny, D. M., McPherson, J., Gibbs, R. A., Fahey, J., Helton, E., Ketteman, M., Madan, A., Rodrigues, S., Sanchez, A., Whiting, M., Madari, A., Young, A. C., Wetherby, K. D., Granite, S. J., Kwong, P. N., Brinkley, C. P., Pearson, R. L., Bouffard, G. G., Blakesly, R. W., Green, E. D., Dickson, M. C., Rodriguez, A. C., Grimwood, J., Schmutz, J., Myers, R. M., Butterfield, Y. S., Griffith, M., Griffith, O. L., Krzywinski, M. I., Liao, N., Morin, R., Palmquist, D., Petrescu, A. S., Skalska, U., Smailus, D. E., Stott, J. M., Schnerch, A., Schein, J. E., Jones, S. J., Holt, R. A., Baross, A., Marra, M. A., Clifton, S., Makowski, K. A., Bosak, S., Malek, J., and Team, M. G. C. P. (2004) The status, quality, and expansion of the NIH full-length cDNA project: the Mammalian Gene Collection (MGC). *Genome Res* **14**, 2121-2127

30. Phan, J., Zdanov, A., Evdokimov, A. G., Tropea, J. E., Peters, H. K., 3rd, Kapust, R. B., Li, M., Wlodawer, A., and Waugh, D. S. (2002) Structural basis for the substrate specificity of tobacco etch virus protease. *The Journal of biological chemistry* **277**, 50564-50572
31. Barb, A. W., Meng, L., Gao, Z., Johnson, R. W., Moremen, K. W., and Prestegard, J. H. (2012) NMR characterization of immunoglobulin G Fc glycan motion on enzymatic sialylation. *Biochemistry-Us* **51**, 4618-4626
32. Vandersall-Nairn, A. S., Merkle, R. K., O'Brien, K., Oeltmann, T. N., and Moremen, K. W. (1998) Cloning, expression, purification, and characterization of the acid a-mannosidase from *Trypanosoma cruzi*. *Glycobiology* **8**, 1183-1194
33. Beckett, D., Kovaleva, E., and Schatz, P. J. (1999) A minimal peptide substrate in biotin holoenzyme synthetase-catalyzed biotinylation. *Protein Sci* **8**, 921-929
34. Pedelacq, J. D., Cabantous, S., Tran, T., Terwilliger, T. C., and Waldo, G. S. (2006) Engineering and characterization of a superfolder green fluorescent protein. *Nat Biotechnol* **24**, 79-88
35. Liu, M., Borgert, A., Barany, G., and Live, D. (2008) Conformational consequences of protein glycosylation: preparation of O-mannosyl serine and threonine building blocks, and their incorporation into glycopeptide sequences derived from alpha-dystroglycan. *Biopolymers* **90**, 358-368
36. Yates, A., Akanni, W., Amode, M. R., Barrell, D., Billis, K., Carvalho-Silva, D., Cummins, C., Clapham, P., Fitzgerald, S., Gil, L., Girón, C. G., Gordon, L., Hourlier, T., Hunt, S. E., Janacek, S. H., Johnson, N., Juettemann, T., Keenan, S., Lavidas, I., Martin, F. J., Maurel, T., McLaren, W., Murphy, D. N., Nag, R., Nuhn, M., Parker, A., Patricio, M., Pignatelli, M., Rahtz, M., Riat, H. S., Sheppard, D., Taylor, K., Thormann, A., Vullo, A., Wilder, S. P., Zadissa, A., Birney, E., Harrow, J., Muffato, M., Perry, E., Ruffier, M., Spudich, G., Trevanion, S. J., Cunningham, F., Aken, B. L., Zerbino, D. R., and Flicek, P. (2016) Ensembl 2016. *Nucleic Acids Research* **44**, D710-D716
37. Sievers, F., Wilm, A., Dineen, D., Gibson, T. J., Karplus, K., Li, W., Lopez, R., McWilliam, H., Remmert, M., Söding, J., Thompson, J. D., and Higgins, D. G. (2011) Fast, scalable generation of high‐quality protein multiple sequence alignments using Clustal Omega. *Molecular Systems Biology* **7**
38. Varki, A., Cummings, R. D., Aebi, M., Packer, N. H., Seeberger, P. H., Esko, J. D., Stanley, P., Hart, G., Darvill, A., Kinoshita, T., Prestegard, J. J., Schnaar, R. L., Freeze, H. H., Marth, J. D., Bertozzi, C. R., Etzler, M. E., Frank, M., Vliegenthart, J. F., Lütteke, T., Perez, S., Bolton, E., Rudd, P., Paulson, J., Kanehisa, M., Toukach, P., Aoki-Kinoshita, K. F., Dell, A., Narimatsu, H.,

York, W., Taniguchi, N., and Kornfeld, S. (2015) Symbol Nomenclature for Graphical Representations of Glycans. *Glycobiology* **25**, 1323-1324

FOOTNOTES

The abbreviations used are: POMGNT2, Protein O-linked mannose β-1,4-N-acetylglucosaminyltransferase 2; POMGNT1, protein O-linked mannose β-1,2-N-acetylglucosaminyltransferase 1; CMD, congenital muscular dystrophy; DGC, dystrophin glycoprotein complex; ECM, extracellular matrix; α-DG, α-Dystroglycan; ER, endoplasmic reticulum; GlcNAc, N-acetyl glucosamine; O-Man, O-mannose.

TABLE 1. Comparison of POMGNT1 and POMGNT2 kinetics with various M1 and M3 synthetic glycopeptide acceptors Asterisk in acceptor sequence indicates the mannosylated threonine residue. Kinetic parameters of Man341 and Man414 with POMGNT2 were not measurable as indicated by the dashed lines.

	Acceptor	Acceptor Sequence	Core Glycan Structure	K_m (mM)	k_{cat} (s^{-1})	k_{cat}/K_m ($M^{-1}s^{-1}$)
POMGNT1	Man317	PKRVRRQIHAT*PTPVTAIGPP	M3	1.2 ± 0.1	13 ± 0.5	10 x 10^3
	Man379	TIRTRGAIIQT*PTLGPIQPTR	M3	2.6 ± 0.4	32 ± 3.3	12 x 10^3
	Man379-ETP	TIETPGAIIQT*PTLGPIQPTR	Modified M3	0.9 ± 0.1	11 ± 0.4	12 x 10^3
	Man341	IQEPPSRIVPT*PTSPAIAPPT	M1	0.1 ± 0.04	1.0 ± 0.1	10 x 10^3
	Man341-RPR	IQRPRSRIVPT*PTSPAIAPPT	Modified M1	3.2 ± 0.7	13 ± 1.5	4.0 x 10^3
	Man414	YVEPT*AV	M1	11 ± 3.0	16 ± 3.3	1.5 x 10^3
POMGNT2	Man317	PKRVRRQIHAT*PTPVTAIGPP	M3	2.2 ± 0.2	12 ± 0.5	5.5 x 10^3
	Man379	TIRTRGAIIQT*PTLGPIQPTR	M3	0.8 ± .04	16 ± 1.4	20 x 10^3
	Man379-ETP	TIETPGAIIQT*PTLGPIQPTR	Modified M3	2.9 ± 0.7	11 ± 1.4	3.8 x 10^3
	Man341	IQEPPSRIVPT*PTSPAIAPPT	M1	--	--	--
	Man341-RPR	IQRPRSRIVPT*PTSPAIAPPT	Modified M1	6.0 ± 1.1	3.3 ± 1.0	0.6 x 10^3
	Man414	YVEPT*AV	M1	--	--	--
	ShortMan379	GAIIQT*PTLGPIQPTR	Modified M3	0.8 ± 0.3	10 ± 1.4	12 x 10^3

FIGURE LEGENDS

FIGURE 1. Core O-Man structures on α-Dystroglycan
A) POMGNT1 is responsible for generating the M1 core glycan structure that can be branched by MGAT5B to generate the M2 core, while POMGNT2 is responsible for generating the M3 core glycan structure.
B) Schematic of known O-mannosylated sites on α-dystroglycan addressed in this study. Thr317 and Thr379 are elaborated with the M3 core glycan structure, while Thr341 and Thr414 are elaborated with M1 core glycan structures that can be further elaborated to core M2 glycan structures. Glycan symbols follow guidelines outlined in (38).

FIGURE 2. Unlike POMGNT1, POMGNT2 exhibits acceptor selectivity
A-B) Radioactive assay of POMGNT1 and POMGNT2 activity with (A) Man341, an M1 acceptor and (B) Man379, an M3 acceptor. Transfer is measured in background corrected disintegrations per minute (DPM). Error bars represent standard error from the mean of 3 replicates.
C-D) FTMS spectra verifying (C) POMGNT1 extended Man341 (1.16 ppm mass accuracy) and (D) POMGNT1 extended Man379 (2.53 ppm mass accuracy). Green circle represents a mannose and the blue square represents an N-acetylglucosamine (38).
E-F) FTMS spectra verifying (E) POMGNT2 Man341 product (1.11 ppm mass accuracy) and (F) POMGNT2 extended Man379 (1.11 ppm mass accuracy). Green circle represents a mannose and the blue square represents an N-acetylglucosamine (38).

FIGURE 3. POMGNT1 transfers to both M1 and M3 acceptors
POMGNT1 kinetics with (A) Man341, (B) Man379, (C) Man414, or (D) Man317 acceptor glycopeptide measured by UDP-Glo assay. Error bars represent standard error from the mean from 3 experiments. See Table 1 for a list of kinetic parameters.

FIGURE 4. POMGNT2 only transfers to M3 acceptors
POMGNT2 kinetics with (A) Man341, (B) Man379, (C) Man414, or (D) Man317 acceptor glycopeptide measured by UDP-Glo assay. Error bars represent standard error from the mean from 3 experiments. See Table 1 for a list of kinetic parameters .

FIGURE 5. A Conserved Consensus Sequence for POMGNT2 Activity
A) Sequence alignment of 21-mer sequences of α-DG centered on known o-mannose sites from human and rabbit (20,21) excluding Thr317 and Thr379. Logo made using Berkeley's WebLogo program.
B) Sequence alignment of 21-mer sequences of α-DG centered on human sites Thr317 and Thr379 from all Ensembl vertebrata with orthologues of DAG1, POMGNT1 or 2 and FKTN or B4GAT1 (total of 59 species, see Experimental Methods for a complete list). Logo made using Berkeley's WebLogo program.

FIGURE 6. A Primary Amino Acid Motif in α-DG is Permissible for POMGNT2 Activity
POMGNT2 kinetics with (A) Man341-RPR and Man341, (B) Man379-ETP and Man379, and (C) ShortMan379 and Man379 acceptor glycopeptide measured by UDP-Glo assay. Error bars represent standard error from the mean from 3 experiments. See Table 1 for a list of kinetic parameters.

Figure 1.

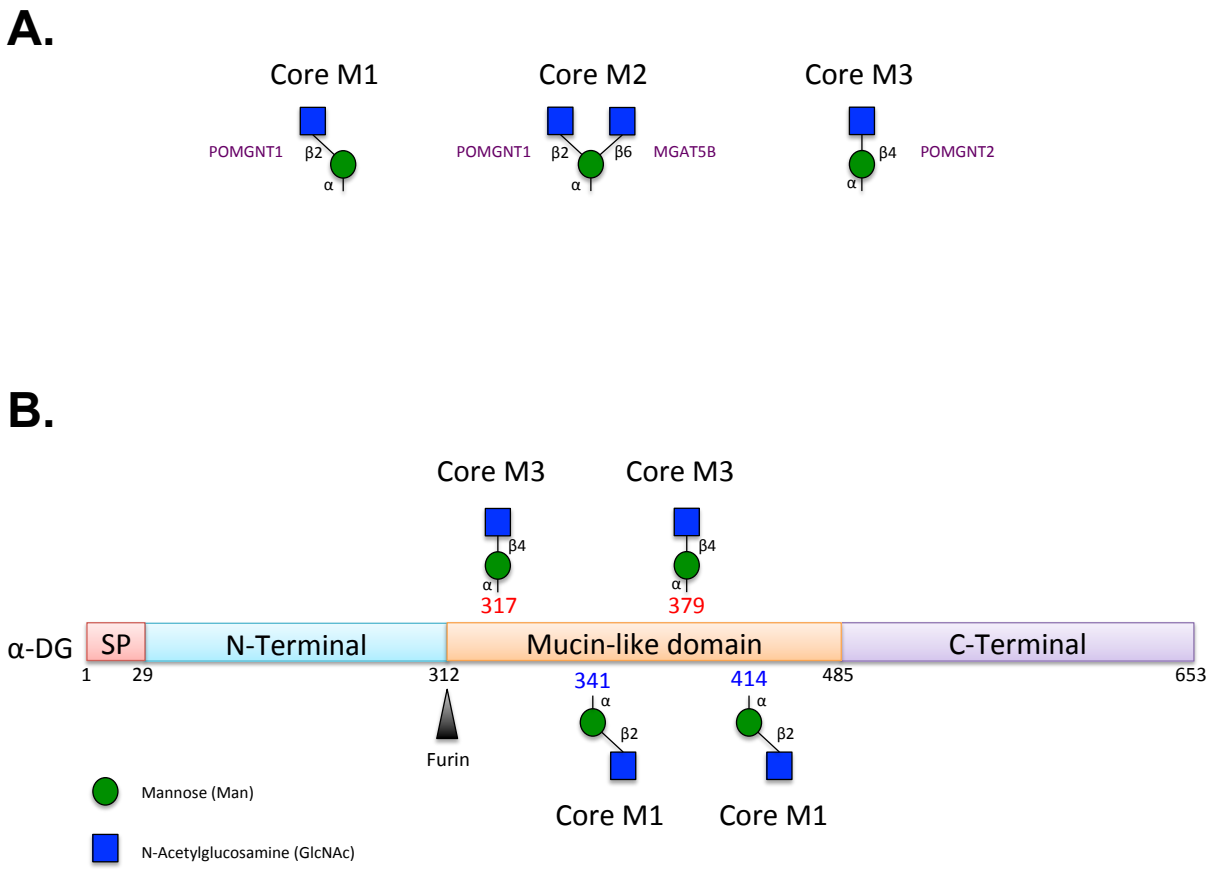

Figure 2.

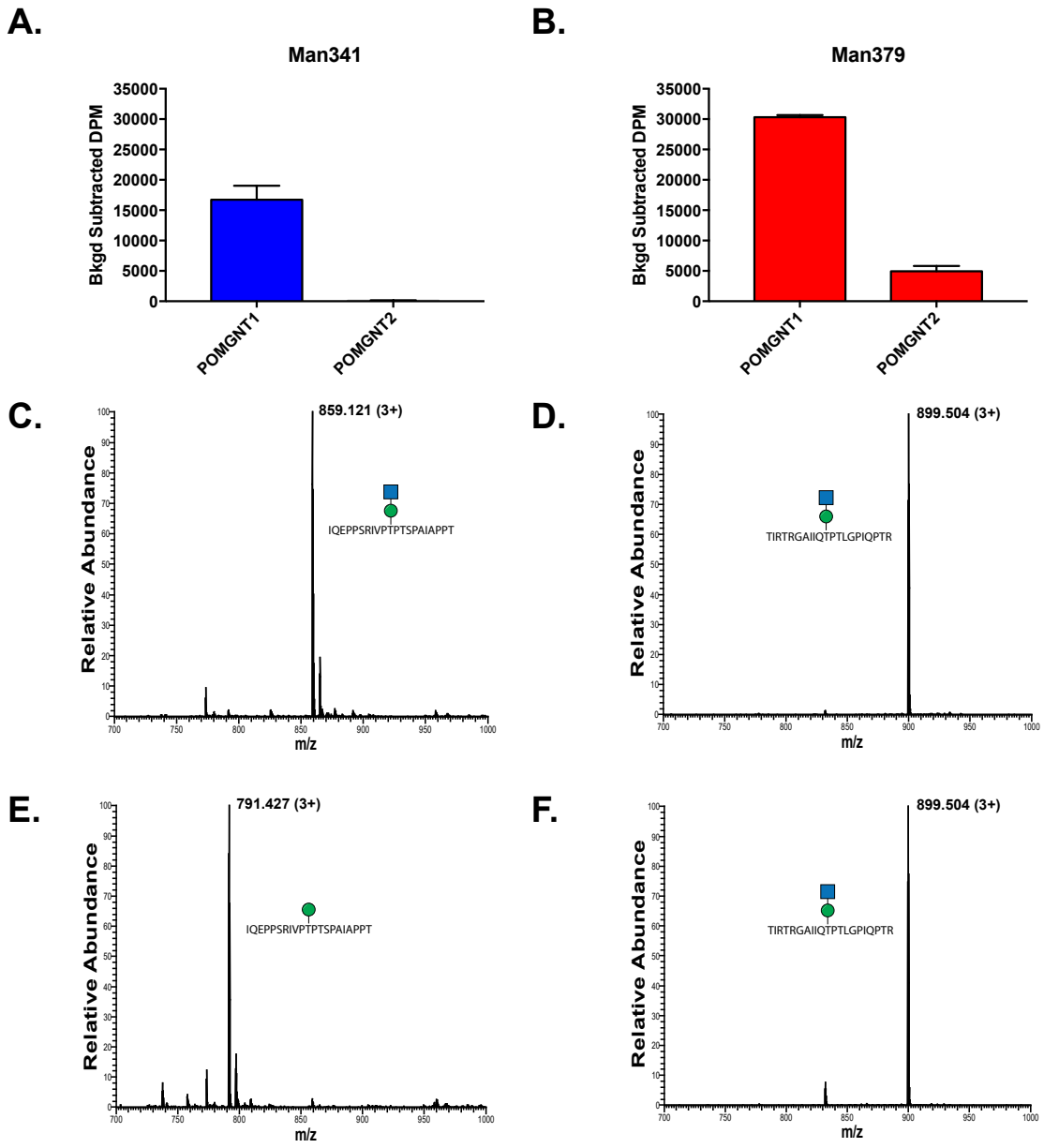

Figure 3.

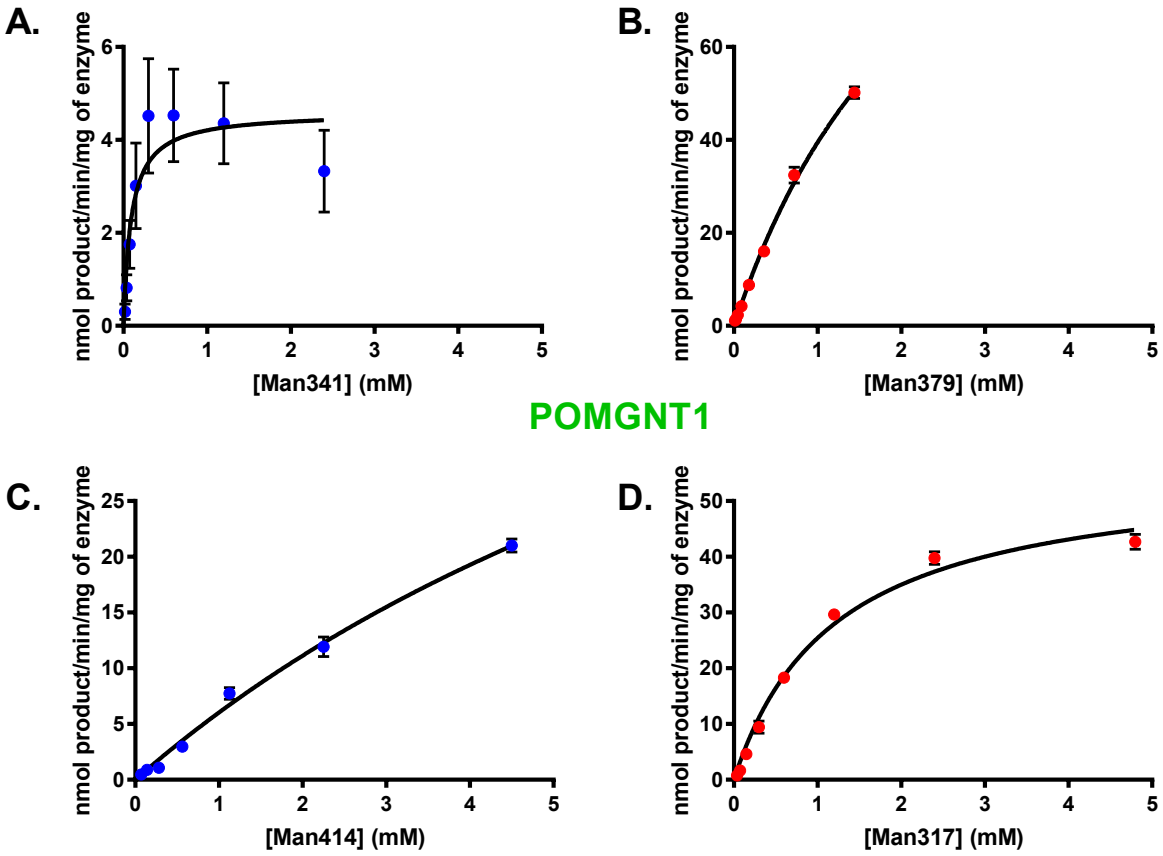

Figure 4.

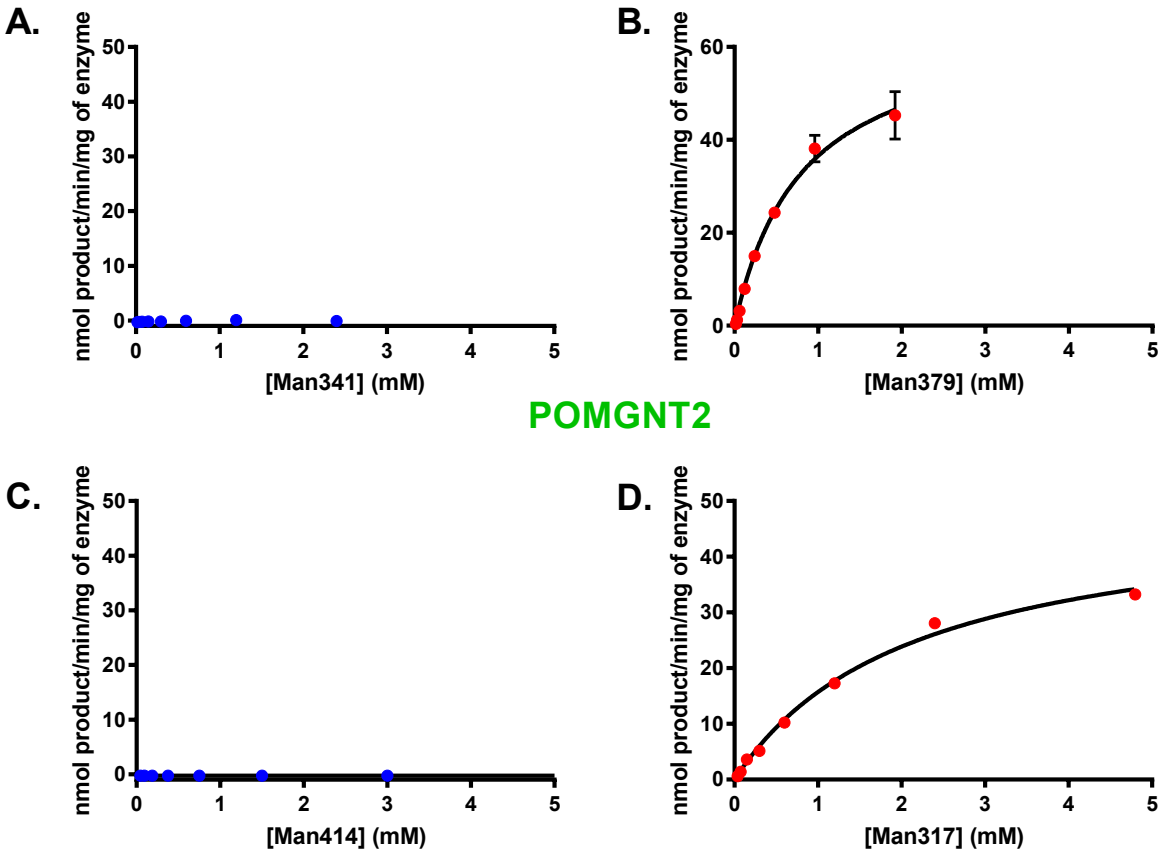

Figure 5.

A.

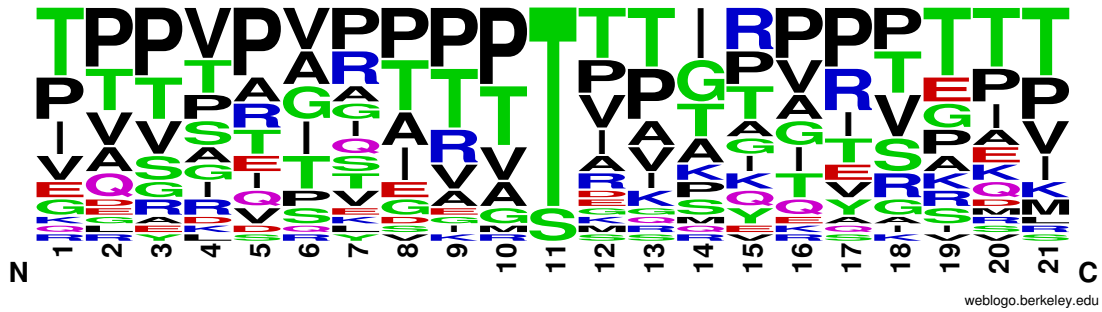

B.

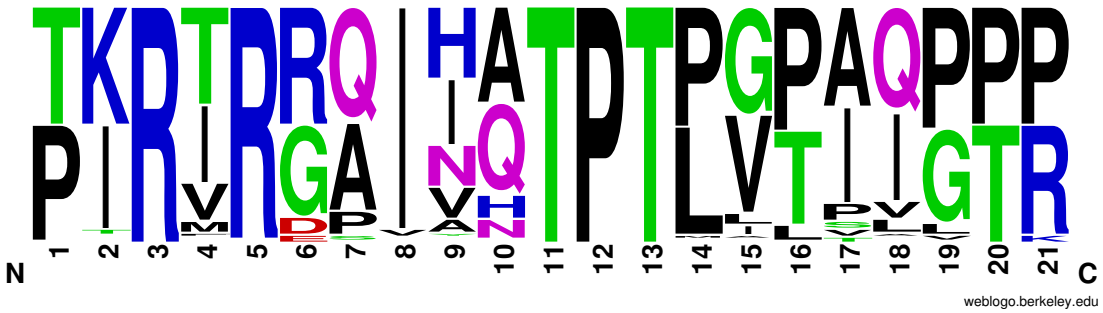

Figure 6.

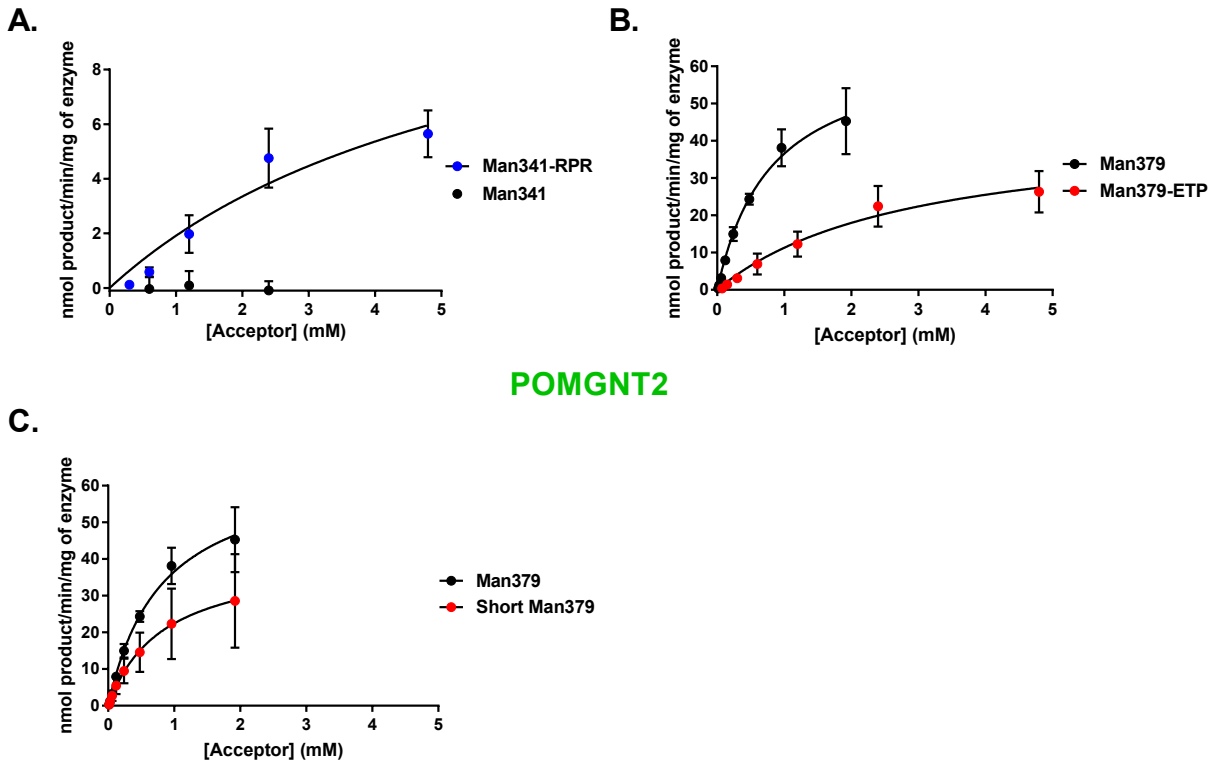

Supplementary Figure 1. (A) HPLC chromatogram (B) and MALDI-TOF spectra of purified glycopeptides Man 317, Man 379, Man 379-ETP, ShortMan379, Man341, Man414, Man341-RPR.

Man317

A.

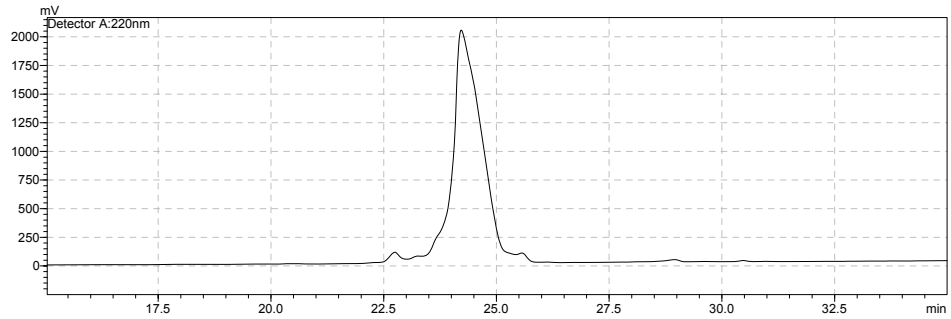
mV
Detector A:220nm
2000
1750
1500
1250
1000
750
500
250
0
17.5
20.0
22.5
25.0
27.5
30.0
32.5
min

B.

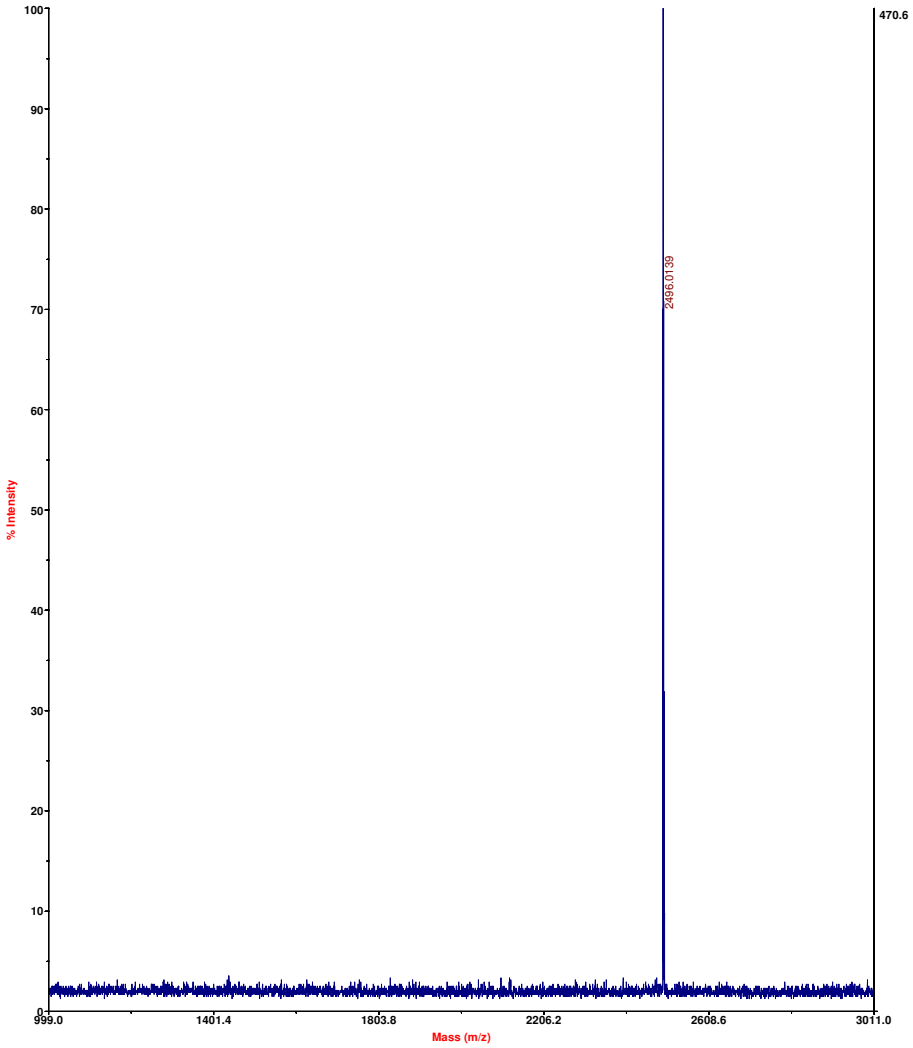
100
90
80
70
60
50
40
30
20
10
0
% Intensity
2496.0139
470.6
999.0
1401.4
1803.8
2206.2
2608.6
3011.0
Mass (m/z)

Man379

A.

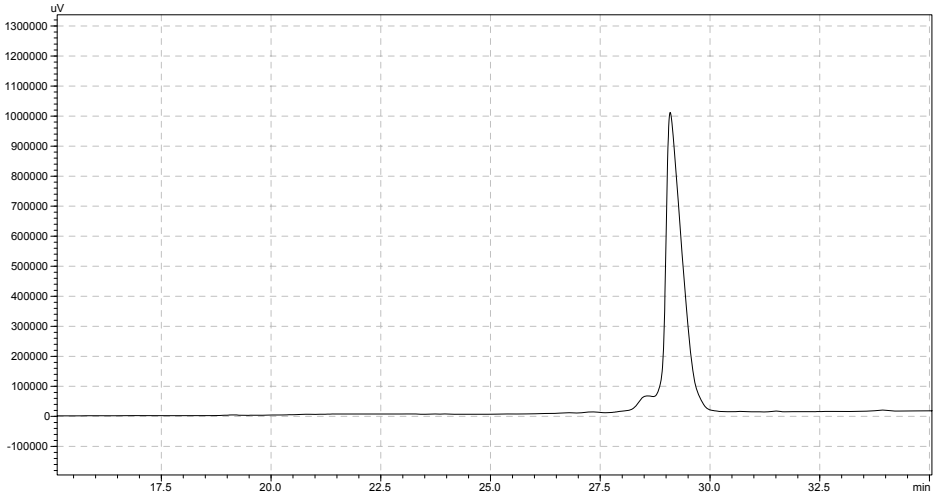
uV
1300000
1200000
1100000
1000000
900000
800000
700000
600000
500000
400000
300000
200000
100000
0
-100000
17.5
20.0
22.5
25.0
27.5
30.0
32.5
min

B.

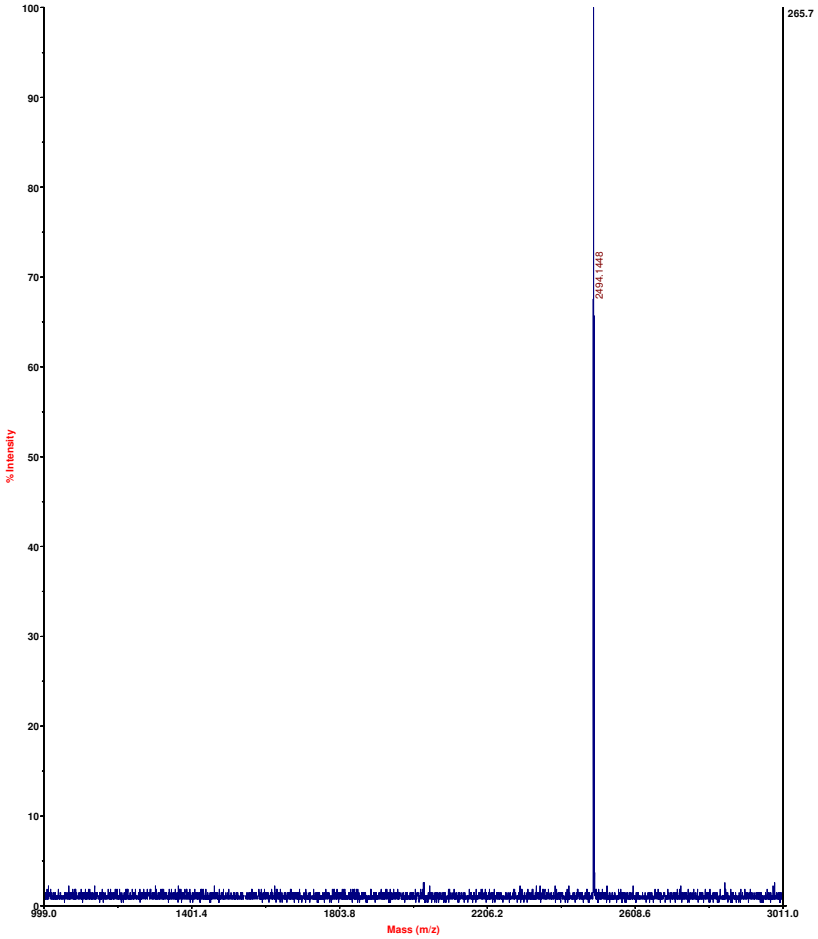
100
90
80
70
60
50
40
30
20
10
0
% Intensity
265.7
2494.1448
999.0
1401.4
1803.8
2206.2
2608.6
3011.0
Mass (m/z)

Man379-ETP

A.

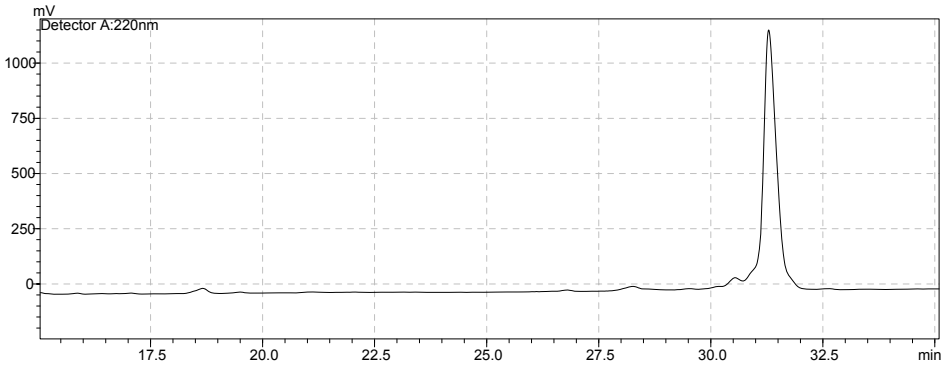

B.

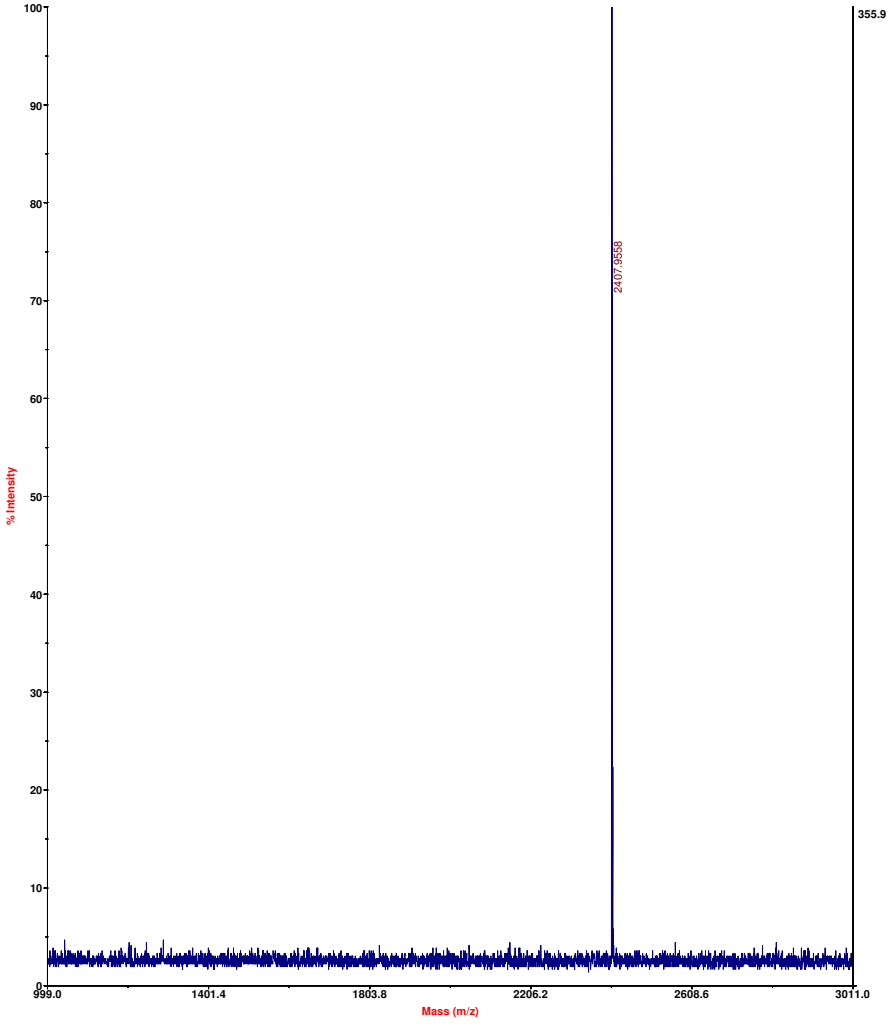

Short Man379

A.

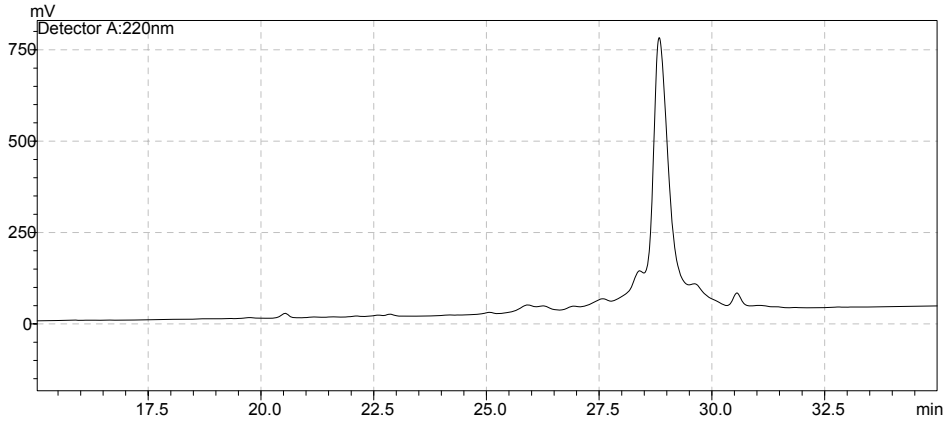

B.

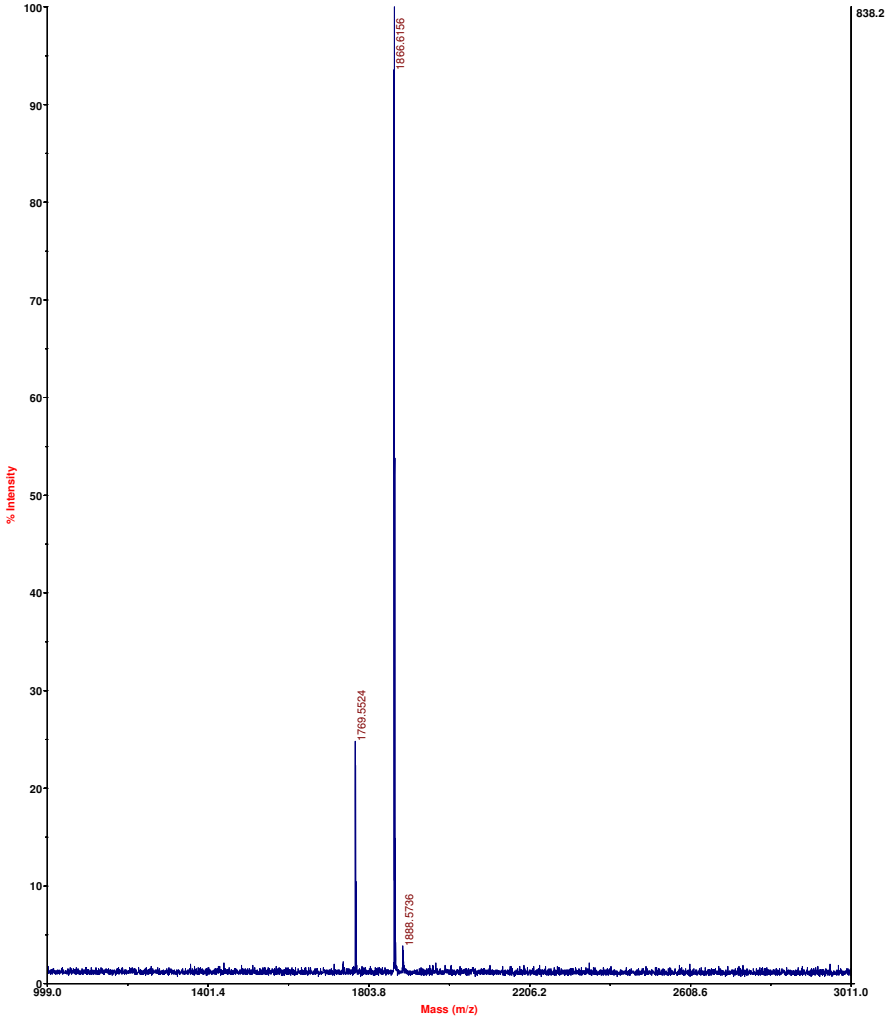

Man341

A.

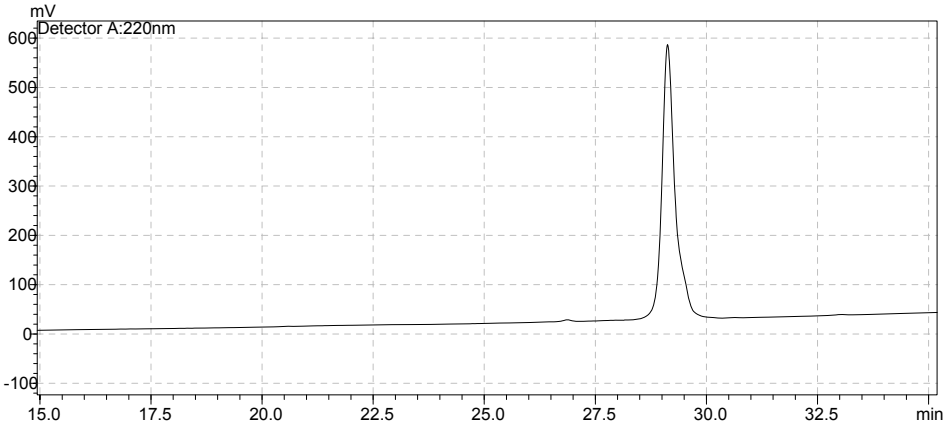
mV
Detector A:220nm
600
500
400
300
200
100
0
-100
15.0
17.5
20.0
22.5
25.0
27.5
30.0
32.5
min

B.

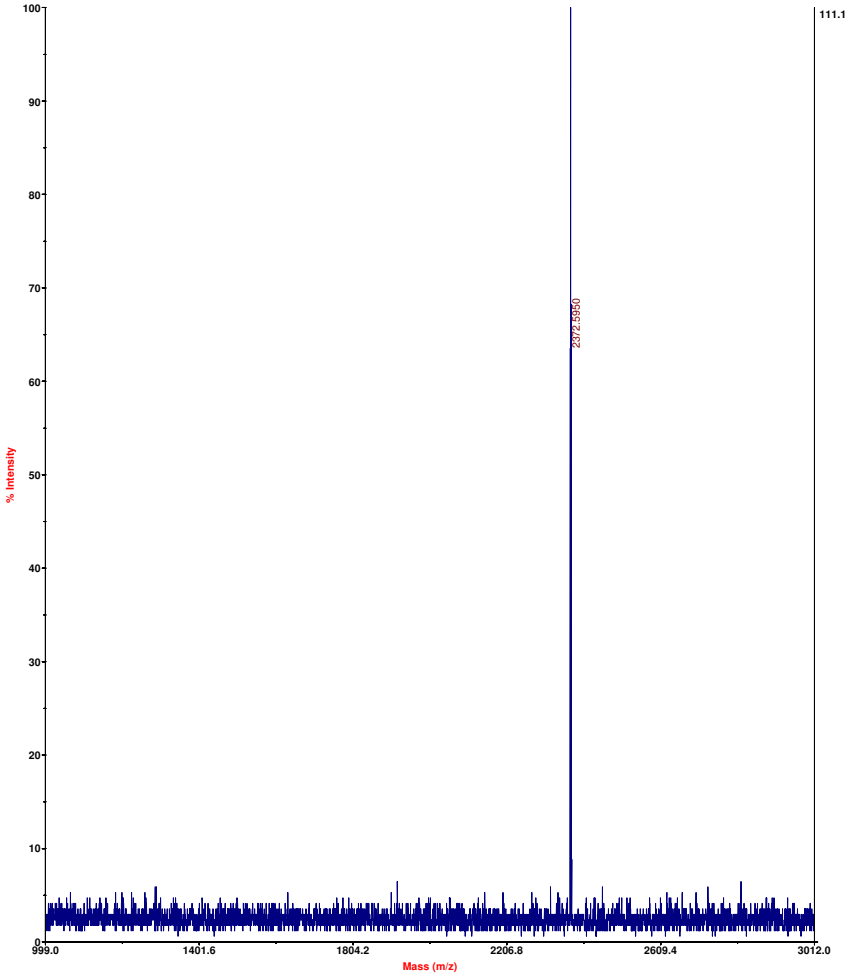
100
90
80
70
60
50
40
30
20
10
0
% Intensity
111.1
2372.5950
999.0
1401.6
1804.2
2206.8
2609.4
3012.0
Mass (m/z)

Man414

A.

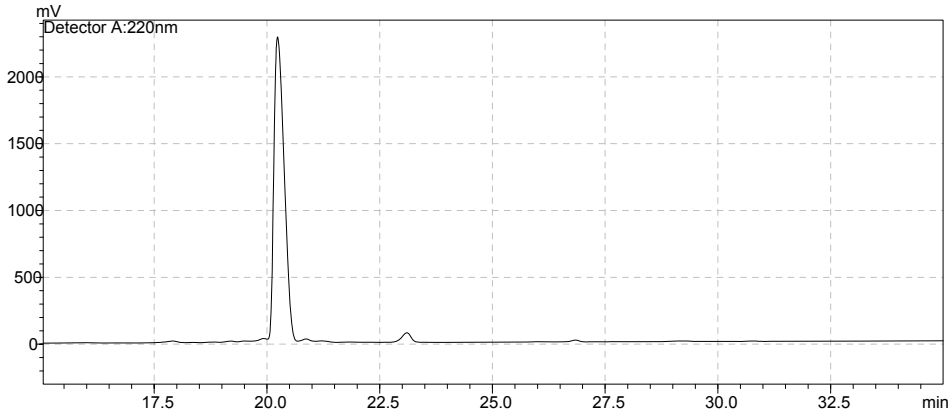
mV
Detector A:220nm
2000
1500
1000
500
0
17.5
20.0
22.5
25.0
27.5
30.0
32.5
min

B.

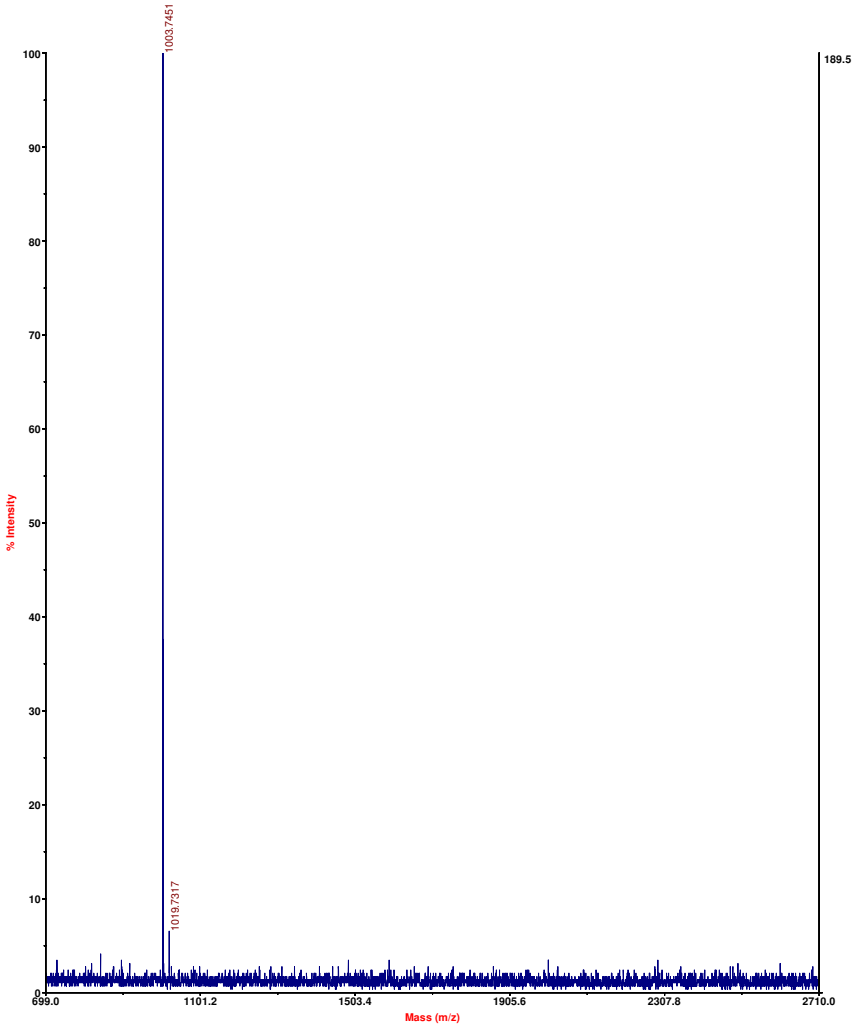
1003.7451
189.5
1018.7317
% Intensity
100
90
80
70
60
50
40
30
20
10
0
699.0
1101.2
1503.4
1905.6
2307.8
2710.0
Mass (m/z)

Man341-RPR

A.

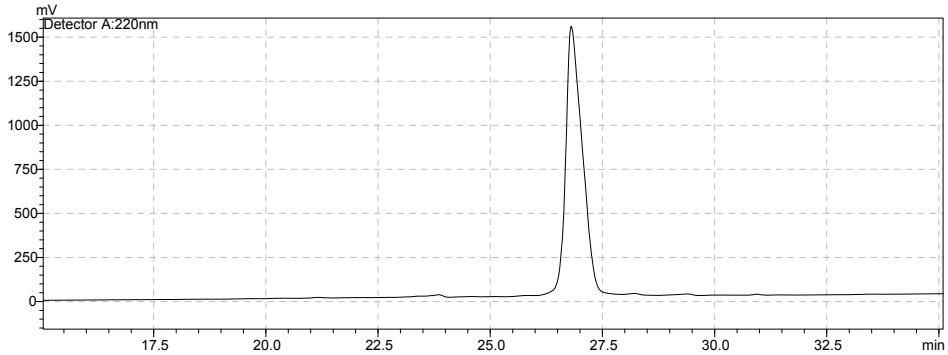

B.

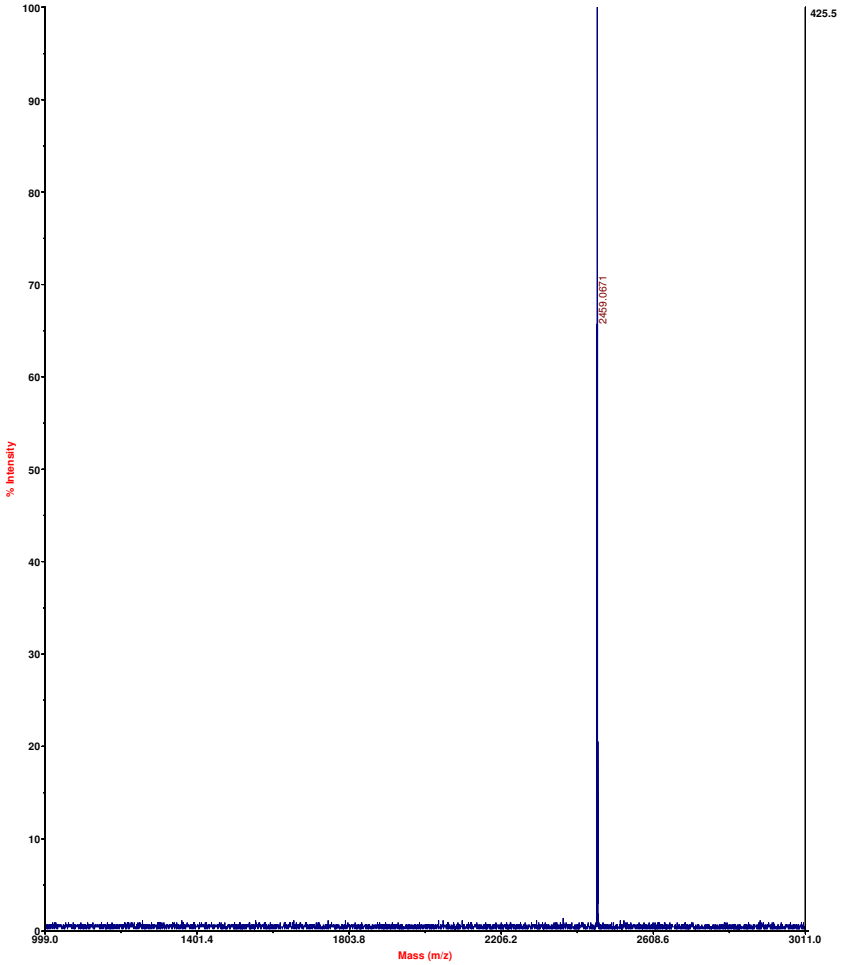

Protein O-linked mannose β-1,4-N-acetylglucosaminyltransferase 2 (POMGNT2) is a gatekeeper enzyme for functional glycosylation of α-dystroglycan

Stephanie M Halmo, Danish Singh, Sneha Patel, Shuo Wang, Melanie Edlin, Geert-Jan Boons, Kelley W Moremen, David Live and Lance Wells

J. Biol. Chem. published online December 8, 2016
